Nanoscale

Accepted Manuscript

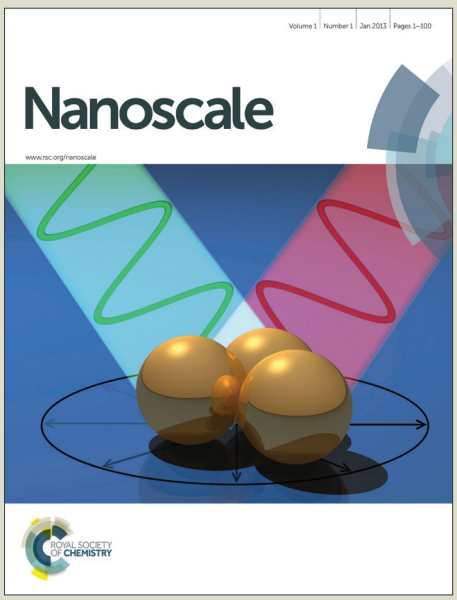

ROYAL SOCIETY OF CHEMISTRY

www.rsc.org/nanoscale

ARTICLE TYPE www. rsc.org/xxxxxx | XXXXXXXX

Controlled Transport of DNA through a Y-shaped Carbon Nanotube in a Solid Membrane†

Binquan Luan,[*a] **Bo Zhou,**[b] **Tien Huynh**[a], and **Ruhong Zhou**[*a]

Received Xth XXXXXXXXXX 20XX, Accepted Xth XXXXXXXXX 20XX
First published on the web Xth XXXXXXXXXX 200X
DOI: 10.1039/b000000x

We investigate the possible ratcheting dynamics of double-stranded DNA (dsDNA) driven through a Y-shaped carbon nanotube (Y-CNT) in a solid membrane, using all-atom molecular dynamics (MD) simulation. By applying constant or alternating biasing voltages, we found that the dsDNA molecule can be unzipped at the junction of the Y-CNT. Because of the energy barrier (a few k_BT per base-pair), the motion of the entire DNA molecule was alternatively in a trapped state or a transiting state. We show that during each transiting state the same number of nucleotides were transported (DNA ratcheting). An analytical theory that is mathematically equivalent to the one for Josephson junctions was then proposed to quantitatively describe the simulation results. The controlled motion of DNA in the Y-CNT is expected to enhance the accuracy of nanopore-based DNA sequencing.

1 Introduction

As a potential next-generation DNA sequencing method, the transport of DNA through a solid-state nanopore has been studied experimentally [1–5] and theoretically [6–8]. Due to the confined geometry of a nanopore, a DNA molecule transits the pore in a single-file manner and the sequence of nucleotides (genetical code) in DNA could be measured electrically [9–11]. The technical challenge lies in the unmatched speeds of the DNA translocation (fast) and the DNA-base sensing (slow). Because of a large conformational fluctuation of DNA in a nanopore [12], typically, multiple measurements of the same nucleotide are required to call the type of a nucleotide [11]. Currently, extensive efforts have been devoted to slowing the DNA translocation through a nanopore, including using the temperature control [13–15], introducing an electro-osmotic flow opposite to the direction of DNA motion [16–18], increasing the viscosity of an electrolyte [14,19], applying an electric field to trap DNA in a nanopore [20,21], controlling functionalized states of a nanopore surface by tuning the pH value of an electrolyte [22], and applying magnetic [23] or optical [24,25] tweezers. Additionally, a ratchet-like motion of DNA is beneficial for the electrical sensing of DNA nucleotides, as demonstrated in experiment of DNA translocation through a protein pore in complex with a DNA polymerase [26,27].

The DNA's transport through a solid-state nanopore is largely affected by its interaction with the pore surface [28]. The motion of DNA is less controllable when unfavorable sticking events occur on the pore surface, causing potential difficulties in sensing DNA nucleotides. Previous experiments show that DNA could be driven through a carbon nanotube (CNT) [29] that has a smooth inner surface and the motion of DNA in a CNT (buried inside a solid-state nanopore) is frictionless [30]. Recently, a CNT-base nanopore was applied to detect modified 5-hydroxymethylcytosin in DNA [31]. Furthermore, the capture-rate of DNA into a CNT-based nanopore could be high because DNA can be spontaneously encapsulated into CNTs [32].

In this paper, we investigated the dynamics of DNA translocation through a Y-shaped CNT (Y-CNT) buried in a solid membrane. The Y-CNT was proposed to separate cat- and anions in an electrolyte [33] and transport signals through confined water molecules inside [34]. Here, a Y-CNT is suggested for transporting, unzipping and ratcheting dsDNA through a Y-CNT. Each unzipped ssDNA strand in a branch of the Y-CNT might be ratcheted forward, because of the trapping energy of 2-3 k_BT from hydrogen bonds in each base-pair (in the unzipped dsDNA segment). We carried out atomistic MD simulations to capture the ratcheting dynamics of DNA motion in a Y-CNT. From the simulation results, a 1D-Langevin-like model was constructed so that it can quantitatively reproduce important features (such as ratcheting) of the dynamics of dsDNA in the Y-CNT nanopore.

2 METHOD

Figure 1a illustrates the simulation system. A solid membrane (SiO_2) separates the *cis*. and *trans*. chambers. A Y-CNT

† Electronic Supplementary Information (ESI) available: The movie showing MD trajectory of dsDNA translocation through a Y-pore (V_{bias}=2 V). See DOI: 10.1039/b000000x/

[a] *IBM research at T. J. Watson Center, 1101 Kitchawan Road, Yorktown Heights, NY, 10598, USA. E-mail: bluan@us.ibm.com; ruhongz@us.ibm.com.*
[b] *Department of Physics and Soft Matter Science Center, Zhejiang University, Hangzhou 310027, China.*

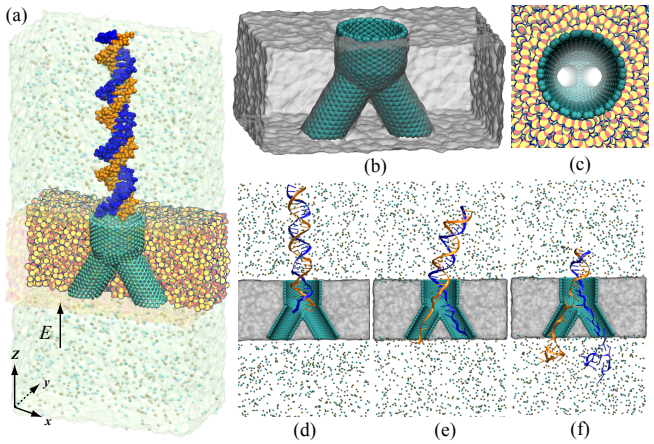

Fig. 1 Illustration of simulated transport of a dsDNA molecule thorugh a Y-pore. a) The set-up of the simulation system. *Si* and *O* atoms in the solid are shown as yellow and red spheres, respectively. The Y-CNT is in the stick representation. Two helical chains of the DNA duplex are colored in orange and blue, repectively. Water is shown transparently. K^+ and Cl^- are shown as tan and cyan sheres. b) An enlarged side view of the Y-pore. c) A top view of the Y-pore. d) A snapshot of the simulated system, showing the entry of the dsDNA molecule into the stem of the Y-pore. e) A snapshot showing the entry of two complementary strands into two branches of the Y-pore. f) A snapshot of the translocation process.

is embedded in the solid membrane (hereafter referred as Y-pore) and connects the *cis*. and *trans*. chambers. In a biasing electric field applied across the system, a DNA molecule (60 base-pairs; random sequence) is driven through the Y-pore. The membrane, pore and DNA are solvated with an 1 M KCl electrolyte.

Figures 1b and 1c show the transparent side-view and perspective top-view of a Y-pore, respectively. The stem part of the Y-CNT has a chirality of (22, 22) and its diameter is about 3.0 nm. Each branch of the Y-CNT has a chirality of (12, 12) and its diameter is about 1.6 nm. Except for the pore size, the CNT's chirality does not affect the dynamics of DNA unzipping/translocation (observed from MD simulations). The angle θ between the symmetry axes of two branches is 60°. To assemble the Y-CNT and SiO_2 together (to form the Y-pore), in an independent MD simulation, the solid membrane was quenched from a high temperature (at which *Si* and *O* atoms were fully mixed) to 300 K; carbon atoms in the Y-CNT were fixed. Subsequently, the complex system was equilibrated at 1 bar and 300 K, with the periodic boundary condition applied in *x*- and *y*- directions only. The thickness *D* of the equilibrated membrane is about 4.8 nm. During this simulation, the BKS force field[35] was used for the amorphous SiO_2 membrane and the force field for the Y-shaped CNT was referred to ref.[34]. Parameters for the van der Waals interaction between C and Si atoms are: ε=0.145 kcal/mol; σ=3.688 Å.

To equilibrate the entire system [Fig. 1a], the CHARMM force field for DNA[36], the TIP3P force field for water[37,38] and standard force field for ions[39] were used in the MD simulation. The Y-CNT was assumed to be functionalized and each carbon atom has a charge of 0.01 e on average. A charged Y-CNT pore lowers the energy barrier for DNA's entry and does not affect the unzipping dynamics of dsDNA significantly. In an independent MD simulation, the unzipping of dsDNA in a neutral pore was also observed.Parameters for the Lennard-Jones interactions between atoms in DNA and fixed carbon atoms (ε_C=-0.01 kcal/mol; $R_{min}/2$=1.992 Å) in the Y-CNT were obtained using the standard CHARMM combination rule. The force field for $SiO2$ solids[40] customized for biological applications was used with reduced van der Waals interactions (ε= -0.01 kcal/mol), so that unzipped ssDNA strands would not stick to the membrane surface. Such surface modification can be achieved in experiment by coating a self-assembled monolayer. The Langevin thermostat was applied to all atoms in the SiO_2 membrane (that were harmonically restrained to their initial positions; spring constant: 20 kcal/mol/$Å^2$) to keep the simulation system at 300 K. Note that it is important not to thermostat ions or molecules that have net momentums in an electric field, because the langevin dynamics can impose extra dragging forces on those ions or molecules. After the system was equilibrated at 1 bar, all following production runs were performed with the NVT ensemble. The size of a typical system measures 11×6×19.7 nm^3. All-atom MD simulations were performed on IBM Bluegene supercomputers using the program NAMD[41]. An external electric field was applied in simulation by turning on the Efield function in NAMD.

3 Results

DNA was initially placed above the membrane as shown in Fig. 1a. After applying a biasing voltage $V_{\rm bias}$ of 0.5 V, the dsDNA was driven into the stem part of the Y-pore [Fig.1d].Only at a higher biasing voltage (e.g. 1.0 V) did the two DNA strands unzip at the junction of the Y-pore and enter their respective branches. The DNA-unzipping force is maximal when each branch tube is filled with a ssDNA fragment [Fig. 1e]. Along the direction of each branch tube, the unzipping force $f_{\rm unzip}$ can be estimated by $q_{\rm eff}V_{\rm bias}/D\cdot\ cos(\theta/2)$, where $q_{\rm eff}$ is the DNA's effective charge. When $V_{\rm bias} \geq$ 0.5 V, the translocation process occurred [Fig. 1f]. Experimentally, the unzipping force of a λ-phage DNA molecule, determined by using an optical tweezer, is about 16 pN[42]. Using $f_{\rm unzip}$=18 pN and $V_{\rm bias}$=1.0 V, we estimated the effective charge of a nucleotide in the ssDNA fragment to be about 0.12 e. This value is close to the experimentally determined effective charges of ssDNA in a small (diameter $\sim$ 1 nm) protein pore, 0.063 e for

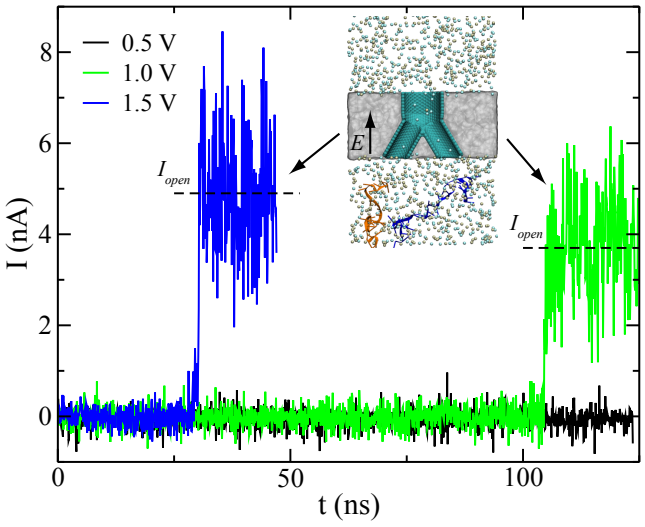

Fig. 2 Ion-currents during and after the DNA translocation. V_{bias}= 0.5 V (black), 1.0 V (green) and 1.5 V (blue). The inset shows a snapshot of the simulation system after the DNA translocation.

transporting ssDNA[43] and 0.1 e for transporting ssDNA from unzipped dsDNA[44].

During the translocation process shown in Fig. 1d-1e, an ionic current through the Y-pore should be physically blocked by the DNA molecule. This is confirmed by analyzing the simulation trajectories and calculating the pore current contributed by motion of ions in a biasing electric field. Figure 2 shows current signals for DNA translocation. During the DNA translocation the pore current was dramatically reduced and after the DNA translocation (see inset of Fig. 2) the pore current was back to an open-pore level. When the biasing voltage was 1.0 V and 1.5 V, the corresponding open-pore currents are 3.7 nA and 4.9 nA respectively [Fig. 2]. When $V_{\rm bias}$=0.5 V, the DNA molecule remained in the state shown in Fig. 1d during the 125-ns simulation. Therefore, the corresponding pore current was always at the blockage level [Fig. 2].

To highlight the dynamics of the DNA translocation through a Y-pore, we show in Fig. 3a the time-dependent N_p, the number of nucleotides coming out of a branch. When $V_{\rm bias}$ is 0.5 V, no nucleotide transited a branch, i.e. N_p=0 [Fig. 3a]. This also suggests that there is an energy barrier to unzip each base-pair in dsDNA. At a high biasing voltage (such as 1.5 V or 2.0 V), N_p increased with time almost linearly. Therefore, the translocation velocity of DNA is nearly constant. At an intermediate biasing voltage (1.0 V), the electric driving process was alternatively in stopped and resumed states. Each state lasted for a random amount of time, indicating a thermally activated process. Therefore, it is possible to ratchet DNA through a Y-pore. In a stop-state for DNA, spikes on yellow and brown lines [Fig. 3a] indicate that the ssDNA moved for-

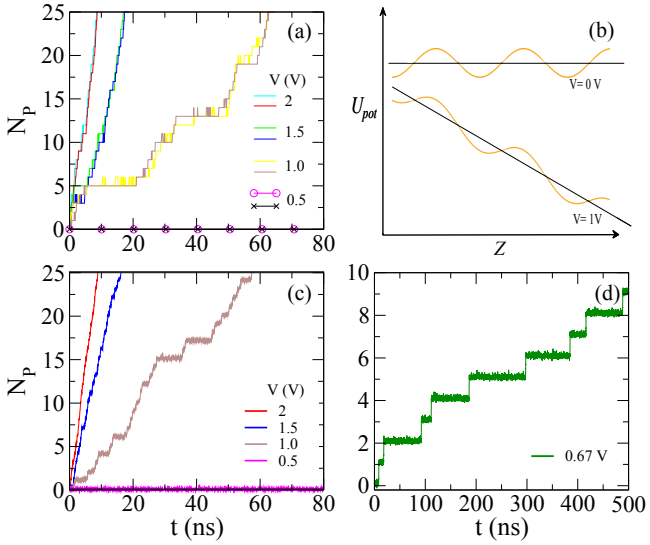

Fig. 3 Electrophoretic motion of the DNA molecule through the Y-pore. a) MD simulation results of time-dependent N_p (number of nucleotides in each DNA strand that have exited the corresponding branch) for two ssDNA strands in two branches. V_{bias} = 0.5, 1, 1.5 and 2 V. b) A schematic plot showing periodic energy-barriers when unzipping two DNA strands, with and without an external biasing voltage. c) Modeled results of time-dependent N_p at same voltages used in simulations. d) The time-dependent N_p from the thoery showing nucleotide-by-nucleotide transport of DNA through the Y-pore when V_{bias}=0.67 V.

ward and backward by one-nucleotide. Note that durations of these spikes are much shorter than the stop (or trapping) time but can add noises in experimentally measured data (e.g. sequencing).

To theoretically characterize the observed dynamics of DNA translocation, we propose a simple model for DNA transport in a Y-pore to account for the complicated translocation processes. As shown in Fig. 3b, periodic potential barriers (2-3 k_BT for hydrogen bonds of base pairing) are assumed during the unzipping process of dsDNA and each potential barrier needs to be overcome before unzipping a base-pair. Thus, the dragging force that prevents the unzipping process can be approximated as $-f_{\max}\sin(2\pi\zeta/d)$, where $f_{\max}$ is the maximum dragging force, ζ is the coordinate along the symmetry axis of a branch and d is the average spacing ($\sim$ 6 Å) between neighboring nucleotides in a branch. Therefore, we use the following equation to treat the driven motion of ssDNA along a branch in a thermal bath and on a periodic potential.

$$m\ddot{\zeta} = -\gamma\dot{\zeta} - f_{\max}\sin(2\pi\zeta/d) + f_{\text{unzip}} + \sqrt{2\gamma k_B T}\xi \qquad (1)$$

where ζ is the ssDNA position along a branch tube; m is the mass of ssDNA and ξ is the δ-correlated white noise. The external forces exerted on ssDNA are hydrodynamic friction force, periodic resisting force and the electric unzipping force. Here, $f_{\max}$=22 pN and f_{unzip}=9, 18, 27, 36 pN, corresponding to biasing voltages of 0.5, 1, 1.5 and 2 V, respectively. Note that this equation is mathematically equivalent to those in the Tomlinson model for friction[45] and models for Josephson Junctions[46]. The ssDNA is in the overdamped regime, as dissipation dominates inertia ($\gamma \gg \sqrt{mk}$).

Without a biasing voltage or in a weak (e.g. 0.5 V) biasing voltage, N_p= 0 during the simulation time [Fig. 3c] and the DNA molecule is stopped (or trapped) at the junction of the Y-pore. With a stronger biasing voltage (such as 1.0 V), the periodic potential is superimposed with a linear potential $-f_{\text{unzip}}\zeta$ and the net potential barrier, as shown in Fig. 3b, is substantially lowered, promoting thermal activations. In Fig. 3c, N_p either increased with time or kept constant, indicating that the DNA molecule was alternatively in a transiting mode or a stopping mode (stop-and-go motion). In the stopping mode, the DNA molecule was trapped in a potential well whose energy barrier could be overcome thermally. With a stronger biasing voltage (e.g. 1.5 and 2 V), the barrier disappears and the driven motion of DNA was steadily sliding as shown in Fig. 3c. These modeled translocation processes agree with the simulated ones shown in Fig. 3a. With a lower biasing voltage of 0.67 V, the energy barrier is relatively higher and it took a longer time for DNA to be thermally activated and move forward by one nucleotide [Fig. 3d]. The modeled result [Fig. 3d] showed that the DNA molecule could be driven forward nucleotide-by-nucleotide (ratcheting mode). However,

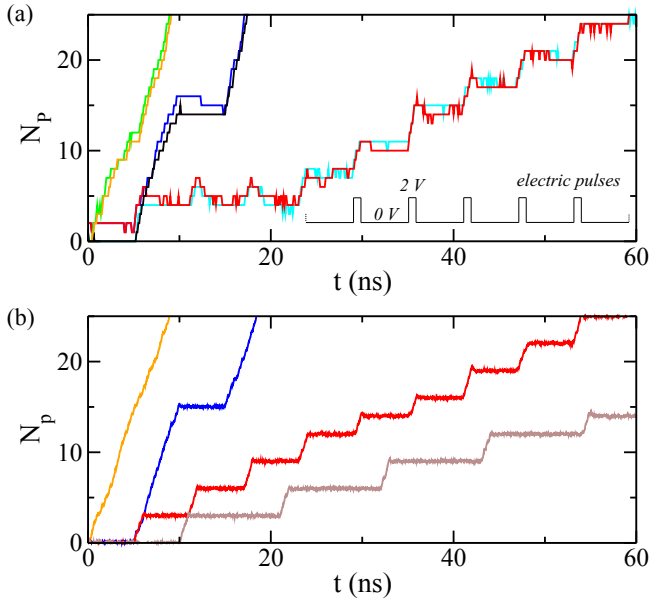

Fig. 4 Transport of DNA in alternating (biasing) voltages. a) Simulated transport-processes for two ssDNA strands in both branches. The inset shows an example of time-dependent biasing voltages. b) Theoretically modeled transport process. τ_{on} and τ_{off} are respectively ∞ and 0 (orange and green), 5 ns and 5 ns (blue and black), 1 ns and 5 ns (red and cyan), 1 ns and 10 ns (brown).

durations when DNA was trapped are not constant and vary dramatically because of thermal activations. The mean trapping time for DNA is proportional to $e^{\Delta U/k_B T}$, where ΔU is the energy barrier for unzipping dsDNA in an external electric field as shown in Fig. 3b. Thus, increasing temperature can reduce the mean trapping time and consequently increase the unzipping rate.

One possible method to actively control the motion of DNA is to apply alternating voltages as shown in the inset of Fig. 4a. During time periods τ_{off}, no biasing voltage was applied and during time periods τ_{on}, a biasing voltage (e.g. 2 V) was applied. Therefore, the motion of DNA could be controlled by periodic voltage signals. In Fig. 4a, simulation results for DNA motion under different voltage signals are presented. When τ_{on}=5 ns and τ_{off}=5 ns, DNA was alternatively trapped for 5 ns (constant N_p) and driven forward for 5 ns. During the moving process, the speed of DNA rarely changed because of the constant dN_p/dt as shown in Fig. 4a. To slow the DNA translocation, in an independent MD simulation, we chose τ_{on}=1 ns and τ_{off}=5 ns. At the beginning (t <20 ns) of the simulation, the inertial effect was observed [Fig.4a]. After that, in each 1-ns driving period, the DNA molecule moved forward about 2-3 nucleotides. For comparison, in Fig. 4a, results for the constant-field driving (τ_{off}=0 ns) are also shown.

The above described processes can also be understood using

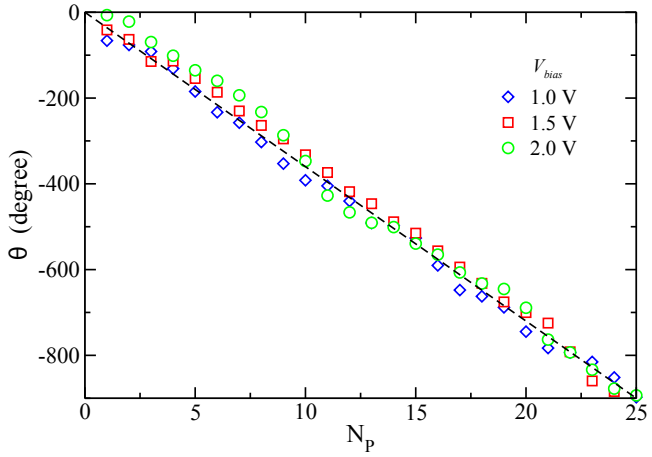

Fig. 5 The dsDNA fragment rotates during the transport at a constant biasing voltage. V_{bias}=1.0 V (diamonds), 1.5 V (squares) and 2.0 V (circles). The slope of the dashed line is -36°.

Eq. 1. According to the alternating electric voltages applied, f_{unzip} was periodically assigned to be 0 and 36 pN. By numerically solving the Eq. 1, modeled processes of DNA translocation in alternating electric voltages, as shown in Fig. 4b, are consistent with simulated ones. Additionally, if increasing τ_{off} to 10 ns [brown line in Fig. 4b], the translocation speed was further reduced and it is possible to have the ratcheting process in which the DNA molecule was alternatively driven forward by 2-3 nucleotides and stalled by 5 ns [red line] or 10 ns [brown line] .

It is worth noting that during the translocation of DNA through a Y-pore, interestingly, the DNA molecule rotated while being driven forward (see movie in supporting material). In Fig. 5, we show the angle which the dsDNA segment rotated about its helical axis vs. number of transported nucleotides N_p. As shown in Fig. 5, simulation data presented in Fig. 3a can be collapsed on the same line. The slope of the line is about 36° per nucleotide transported, corresponding to the rotation angle per base-pair in dsDNA.

4 Conclusions

In summary, we have investigated the ratcheting motion of dsDNA inside a Y-pore and developed an analytical model to uncover the mechanism of the ratcheting dynamics. Our simulations show, when driven by a weak biasing voltage, dsDNA can be forced to transit the Y-pore in a stop-and-go fashion. When applying alternative biasing voltages, the ratcheting process of dsDNA through the Y-pore become possible. Simulation results were quantitatively compared with theoretical predictions from the analytical model. The ratcheting dynamics is essential for sequencing DNA in a nanopore because the nucleotide near a sensor could be called accurately during the "stop" phase. Experimentally, a dsDNA molecule was demonstrated to be electrically driven into a protein pore and was unzipped so that only one DNA strand can pass the constriction site of the protein pore[44]. The unzipping dynamics of dsDNA in a Y-pore is different and allows the transport of each DNA strand in a CNT branch. Potentially, it is possible to sequence complementary DNA strands simultaneously, improving the sequencing accuracy.

The suggested translocation of DNA through a Y-CNT pore could be permissible in experiment, because both the fabrication of Y-CNT[47] and translocation of DNA through a CNT[29] have been experimentally demonstrated. We expect that after being realized in experiment the controlled motion of DNA described above could benefit the DNA-sequencing technology based on nanopores[3].

References

1 J. Li, M. Gershow, D. Stein, E. Brandin and J. A. Golovchenko, *Nature Mater.*, 2003, **2**, 611–615.
2 C. Dekker, *Nature Nanotech.*, 2007, **2**, 209 – 215.
3 D. Branton, D. Deamer, A. Marziali, H. Bayley, S. Benner, T. Butler, M. Di Ventra, S. Garaj, A. Hibbs, X. Huang and et al., *Nature Biotech.*, 2008, **26**, 1146–1153.
4 B. Venkatesan and R. Bashir, *Nature Nanotech.*, 2011, **6**, 615–624.
5 M. Wanunu, T. Dadosh, V. Ray, J. Jin, L. McReynolds and M. Drndić, *Nature Nanotech.*, 2010, **5**, 807–814.
6 K. Luo, T. Ala-Nissila, S. Ying and A. Bhattacharya, *Phys. Rev. Lett.*, 2008, **100**, 58101.
7 C. T. A. Wong and M. Muthukumar, *J. Chem. Phys.*, 2007, **126**, 164903.
8 D. Lubensky and D. Nelson, *Biophys. J.*, 1999, **77**, 1824–1838.
9 J. Lagerqvist, M. Zwolak and M. D. Ventra, *Nano Lett.*, 2006, **6**, 779–782.
10 S. Chang, J. He, A. Kibel, M. Lee, O. Sankey, P. Zhang and S. Lindsay, *Nature Nanotech.*, 2009, **4**, 297–301.
11 M. Tsutsui, M. Taniguchi, K. Yokota and T. Kawai, *Nature Nanotech.*, 2010, **5**, 286–290.
12 S. Markosyan, P. M. De Biase, L. Czapla, O. Samoylova, G. Singh, J. Cuervo, D. P. Tieleman and S. Y. Noskov, *Nanoscale DOI:10.1039/C3NR06559F*, 2014.
13 A. Meller, L. Nivon, E. Brandin, J. Golovchenko and D. Branton, *Proc. Natl. Acad. Sci. USA*, 2000, **97**, 1079–1084.
14 D. Fologea, J. Uplinger, B. Thomas, D. S. McNabb and J. Li, *Nano Lett.*, 2005, **5**, 1734–1737.

15 Y. He, M. Tsutsui, R. H. Scheicher, F. Bai, M. Taniguchi and T. Kawai, *ACS nano*, 2012, **7**, 538–546.

16 B. Q. Luan and A. Aksimentiev, *Phys. Rev. E*, 2008, **78**, 021912.

17 S. van Dorp, U. Keyser, N. Dekker, C. Dekker and S. Lemay, *Nature Phys.*, 2009, **5**, 347–351.

18 N. Di Fiori, A. Squires, D. Bar, T. Gilboa, T. D. Moustakas and A. Meller, *Nature Nanotech.*, 2013, **8**, 946–951.

19 B. Luan, D. Wang, R. Zhou, S. Harrer, H. Peng and G. Stolovitzky, *Nanotechnology*, 2012, **23**, 455102.

20 G. Sigalov, J. Comer, G. Timp and A. Aksimentiev, *Nano Lett.*, 2008, **8**, 56–63.

21 B. Luan, H. Peng, S. Polonsky, S. Rossnagel, G. Stolovitzky and G. Martyna, *Phys. Rev. Lett.*, 2010, **104**, 238103.

22 B. N. Anderson, M. Muthukumar and A. Meller, *ACS nano*, 2012, **7**, 1408–1414.

23 H. Peng and X. Ling, *Nanotechnology*, 2009, **20**, 185101–185108.

24 U. Keyser, B. Koeleman, S. van Dorp, D. Krapf, R. Smeets, S. Lemay, N. Dekker and C. Dekker, *Nature Phys.*, 2006, **2**, 473–477.

25 E. Trepagnier, A. Radenovic, D. Sivak, P. Geissler and J. Liphardt, *Nano Lett.*, 2007, **7**, 2824–2830.

26 E. Manrao, I. Derrington, A. Laszlo, K. Langford, M. Hopper, N. Gillgren, M. Pavlenok, M. Niederweis and J. Gundlach, *Nature Biotech.*, 2012, **30**, 349–353.

27 G. M. Cherf, K. R. Lieberman, H. Rashid, C. E. Lam, K. Karplus and M. Akeson, *Nature Biotech.*, 2012, **30**, 344–348.

28 M. Wanunu, J. Sutin, B. McNally, A. Chow and A. Meller, *Biophys. J.*, 2008, **95**, 4716–4725.

29 H. Liu, J. He, J. Tang, H. Liu, P. Pang, D. Cao, P. Krstic, S. Joseph, S. Lindsay and C. Nuckolls, *Science*, 2010, **327**, 64.

30 V. Lulevich, S. Kim, C. P. Grigoropoulos and A. Noy, *Nano Lett.*, 2011, **11**, 1171–1176.

31 L. Liu, C. Yang, K. Zhao, J. Li and H. Wu, *Nature Comms. doi:10.1038/ncomms3989*, 2014.

32 H. Gao, Y. Kong, D. Cui and C. S. Ozkan, *Nano Lett.*, 2003, **3**, 471–473.

33 J. H. Park, S. B. Sinnott and N. Aluru, *Nanotechnology*, 2006, **17**, 895.

34 Y. Tu, P. Xiu, R. Wan, J. Hu, R. Zhou and H. Fang, *Proc. Natl. Acad. Sci. USA*, 2009, **106**, 18120–18124.

35 B. van Beest, G. Kramer and R. van Santen, *Phys. Rev. Lett.*, 1990, **64**, 1955–1958.

36 A. MacKerell, Jr., D. Bashford, M. Bellott, R. L. Dunbrack, Jr., J. Evanseck, M. J. Field, S. Fischer, J. Gao, H. Guo, S. Ha, D. Joseph, L. Kuchnir, K. Kuczera, F. T. K. Lau, C. Mattos, S. Michnick, T. Ngo, D. T. Nguyen, B. Prodhom, I. W. E. Reiher, B. Roux, M. Schlenkrich, J. Smith, R. Stote, J. Straub, M. Watanabe, J. Wiorkiewicz-Kuczera, D. Yin and M. Karplus, *J. Phys. Chem. B*, 1998, **102**, 3586–3616.

37 W. L. Jorgensen, J. Chandrasekhar, J. D. Madura, R. W. Impey and M. L. Klein, *J. Chem. Phys.*, 1983, **79**, 926–935.

38 E. Neria, S. Fischer and M. Karplus, *J. Chem. Phys.*, 1996, **105**, 1902.

39 D. Beglov and B. Roux, *J. Chem. Phys.*, 1994, **100**, 9050–9063.

40 E. R. Cruz-Chu, A. Aksimentiev and K. Schulten, *J. Phys. Chem. B*, 2006, **110**, 21497–21508.

41 J. C. Phillips, *et.al.*, *J. Comp. Chem.*, 2005, **26**, 1781.

42 U. Bockelmann, P. Thomen, B. Essevaz-Roulet, V. Viasnoff and F. Heslot, *Biophys. J.*, 2002, **82**, 1537–1553.

43 S. Henrickson, M. Misakian, B. Robertson and J. J. Kasianowicz, *Phys. Rev. Lett.*, 2000, **85**, 3057–3060.

44 A. F. Sauer-Budge, J. A. Nyamwanda, D. K. Lubensky and D. Branton, *Phys. Rev. Lett.*, 2003, **90**, 238101.

45 M. O. Robbins, *Jamming and Rheology*, Taylor & Francis, London, 2001.

46 D. McCumber, *J. Appl. Phys.*, 1968, **39**, 3113.

47 J. Li, C. Papadopoulos and J. Xu, *Nature*, 1999, **402**, 253–254.